



Published in final edited form as:

*Nat Genet.* ; 43(8): 776–784. doi:10.1038/ng.891.

## A Transition Zone Complex Regulates Mammalian Ciliogenesis and Ciliary Membrane Composition

Francesc R. Garcia-Gonzalo<sup>1,2,\*</sup>, Kevin C. Corbit<sup>1,2,\*</sup>, María Salomé Sirerol-Piquer<sup>3</sup>, Gokul Ramaswami<sup>4,5</sup>, Edgar A. Otto<sup>4,5</sup>, Thomas R. Noriega<sup>1</sup>, Allen D. Seol<sup>1,2</sup>, Jon F. Robinson<sup>6,7</sup>, Christopher L. Bennett<sup>6,7</sup>, Dragana J. Josifova<sup>8</sup>, José Manuel García-Verdugo<sup>3,9</sup>, Nicholas Katsanis<sup>6,7</sup>, Friedhelm Hildebrandt<sup>4,5,10</sup>, and Jeremy F. Reiter<sup>1,2</sup>

<sup>1</sup> Department of Biochemistry and Biophysics, University of California, San Francisco, San Francisco, CA 94158, USA

<sup>2</sup> Cardiovascular Research Institute, University of California, San Francisco, San Francisco, CA 94158, USA

<sup>3</sup> Laboratorio de Morfología Celular, Unidad Mixta CIPF-UVEG, CIBERNED, Valencia, Spain

<sup>4</sup> Department of Pediatrics, University of Michigan, Ann Arbor, MI 48109, USA

<sup>5</sup> Department of Human Genetics, University of Michigan, Ann Arbor, MI 48109, USA

<sup>6</sup> Center for Human Disease Modeling, Department of Cell Biology, Duke University, Durham, NC 27710, USA

<sup>7</sup> Department of Pediatrics, Duke University, Durham, NC 27710, USA

<sup>8</sup> Department of Clinical Genetics, Guy's Hospital, London, SE1, 9RT, UK

<sup>9</sup> Department of Comparative Neurobiology, Cavanilles Institute of Biodiversity and Evolutionary Biology, University of Valencia, Spain

<sup>10</sup> Howard Hughes Medical Institute, Chevy Chase, MD 20815, USA

### Abstract

Mutations in genes encoding ciliary components cause ciliopathies, but how many of these mutations disrupt ciliary function is unclear. We investigated Tectonic1 (Tctn1), a regulator of mouse Hedgehog signaling, and found that it is essential for ciliogenesis in some, but not all, tissues. Cell types that do not require Tctn1 for ciliogenesis require it to localize select membrane-associated proteins to the cilium, including Arl13b, AC3, Smoothed and Pkd2. Tctn1 forms a

---

Users may view, print, copy, download and text and data-mine the content in such documents, for the purposes of academic research, subject always to the full Conditions of use: [http://www.nature.com/authors/editorial\\_policies/license.html#terms](http://www.nature.com/authors/editorial_policies/license.html#terms)

\*These authors contributed equally to this work.

#### SUPPLEMENTAL INFORMATION

Supplemental information includes eight figures and one table.

#### AUTHOR CONTRIBUTIONS

F.R.G-G. and K.C.C. performed most experiments and wrote the manuscript. M.S.S did most electron microscopy, supervised by J.M.G-V. Human genetics were supervised by F.H. and N.K. and performed by G.R., E.A.O., D.J.J., C.L.B. and J.F.Robinson. T.R.N performed the gel filtration chromatography. A.D.S. helped with mouse experiments. J.F.Reiter wrote the manuscript and supervised the work.

complex with multiple ciliopathy proteins associated with Meckel (MKS) and Joubert (JBTS) syndromes, including Mks1, Tmem216, Tmem67, Cep290, B9d1, Tctn2, and Cc2d2a. Components of the Tectonic ciliopathy complex colocalize at the transition zone, a region between the basal body and ciliary axoneme. Like Tctn1, loss of complex components Tctn2, Tmem67 or Cc2d2a causes tissue-specific defects in ciliogenesis and ciliary membrane composition. Consistent with a shared function for complex components, we identified a mutation in *TCTN1* that causes JBTS. Thus, a transition zone complex of MKS and JBTS proteins regulates ciliary assembly and trafficking, suggesting that transition zone dysfunction is the cause of these ciliopathies.

## INTRODUCTION

Cilia are microtubule-based cell surface projections, likely possessed by the eukaryotic ancestor<sup>1</sup>. Some mammalian cells possess motile cilia, whose functions include pulmonary mucous clearance and left-right axis determination. In contrast, most primary cilia are immotile, instead functioning in signal transduction during embryogenesis and adult tissue homeostasis<sup>2</sup>.

An early ciliogenic event is the docking of the mother centriole to a vesicle<sup>3</sup>. Following docking, the centriole extends an axoneme that invaginates the vesicle. Fusion of the vesicle with the plasma membrane exposes the nascent cilium to the extracellular environment. Vesicle trafficking is required for ciliogenesis, and thereafter contributes lipids and transmembrane proteins to the ciliary membrane<sup>4</sup>.

Once transported to the ciliary base, ciliary-bound transmembrane proteins must cross the transition zone, a region between the basal body and axoneme. Although little is known about the transition zone, three nephronophthisis (NPHP)-associated proteins, Nphp1, Nphp4 and Rpgrip11, form a complex that localizes to this compartment<sup>5</sup>. Furthermore, transition zone components regulate ciliary protein composition in *Chlamydomonas*, *C. elegans*, and mammalian cells<sup>6-8</sup>.

Ciliary dysfunction underlies a group of diseases, termed ciliopathies, that include JBTS, characterized by cerebellar and brainstem malformations, MKS, characterized by occipital encephalocele, kidney cysts and polydactyly, and NPHP, characterized by medullary kidney cysts<sup>9-10</sup>. The genes underlying these ciliopathies display extensive allelism. For example, mutations in six MKS genes, *TMEM216*, *TMEM67*, *CEP290*, *RPGRIP1L*, *CC2D2A* and *TCTN2*, also cause JBTS or COACH, which resembles JBTS but includes liver fibrosis<sup>5,9-11</sup>. Some of these loci also cause or modify the manifestations of ciliopathies such as Bardet-Biedl syndrome (BBS), characterized by obesity, polydactyly and retinitis pigmentosa<sup>10-13</sup>.

Polycystic kidney disease (PKD), a common ciliopathy, is caused by mutations in ciliary transmembrane proteins, including Pkd2<sup>9-10</sup>. Targeting of transmembrane proteins to cilia involves ciliary localization sequences (CLSs)<sup>4</sup>. For example, Pkd2 relies upon an amino-terminal RVxP sequence, whereas Rhodopsin uses a carboxy-terminal VxPx motif<sup>14-15</sup>. Other CLSs, such as that of SSTR3, bind the BBSome, a protein complex involved in

BBS<sup>16-18</sup>. The BBSome acts as a membrane coat trafficking G-protein-coupled receptors (GPCRs) to the cilium<sup>16</sup>. Despite its important role in GPCR targeting, the BBSome is not required for ciliogenesis in most tissues<sup>19</sup>.

Abrogating vertebrate ciliogenesis disrupts Hedgehog (Hh) signaling, resulting in embryonic neural tube dorsalization and polydactyly<sup>2</sup>. Many Hh pathway components, including Patched1 (Ptch1), Smoothed (Smo), Sufu, and Gli transcription factors, localize to cilia, and ciliary translocation of Smo is required to robustly activate the pathway<sup>2,20</sup>. Cilia also participate in other pathways, such as Pdgfr- $\alpha$ , Wnt and mTOR signaling<sup>2,4,21</sup>.

We previously described a novel gene, *Tctn1*, that modulates mouse Hh signal transduction<sup>22</sup>. *Tctn1* belongs to a family of signal sequence-containing proteins conserved among eukaryotes that generate cilia or flagella. We demonstrate that *Tctn1* forms a membrane-spanning transition zone complex with JBTS and MKS proteins, and identify human *TCTN1* as a novel JBTS gene. The Tectonic ciliopathy complex controls ciliogenesis and ciliary protein composition, suggesting that JBTS, COACH and MKS result from transition zone dysfunction.

## RESULTS

### **Tctn1 is required for ciliogenesis in a tissue-dependent manner**

We previously demonstrated that *Tctn1* is expressed specifically in the node of late headfold-stage mouse embryos and is required for correct establishment of left-right asymmetry<sup>22</sup>. Consistently, nodal flow and left lateral plate induction of *Nodal* gene expression are disrupted in *Tctn1*<sup>-/-</sup> mouse embryos (Figure S1a and data not shown). Because left-right axis determination depends on leftward flow generated by nodal cilia<sup>22</sup>, we examined these cilia in *Tctn1*<sup>-/-</sup> embryos. Staining of E8.5 embryonic nodes for Arl13b, a ciliary membrane-associated protein<sup>23-24</sup>, revealed abundant cilia in wild type nodes, but not *Tctn1*<sup>-/-</sup> nodes (Figure 1a). Scanning electron microscopy (SEM) confirmed the absence of cilia in *Tctn1*<sup>-/-</sup> nodes, and transmission electron microscopy (TEM) demonstrated that basal bodies of mutant node cells attach to the plasma membrane but fail to extend axonemes (Figures 1b-c).

In addition to left-right axis specification, *Tctn1* is required for Sonic hedgehog (Shh) patterning of the ventral neural tube<sup>22</sup>. Cilia are essential for interpreting Shh signals during vertebrate neural development<sup>2</sup>. Immunostaining of wild type and *Tctn1*<sup>-/-</sup> E10.5 neural tubes for Arl13b and  $\gamma$ -tubulin, a basal body component, revealed a normal number and localization of basal bodies, coupled with a dramatic reduction in the number of cilia (Figure 1d). By SEM, cilia were numerous in control, but scarce in *Tctn1*<sup>-/-</sup> neural tubes. Of the few neural cilia that formed in mutants, most were short and bulbous, while some displayed swellings (Figure 1e). TEM of *Tctn1*<sup>-/-</sup> neural tubes confirmed that basal bodies dock to the apical membrane in the absence of *Tctn1*, but mostly fail to extend axonemes (Figures 1f and S1b).

Thus, *Tctn1* mutant phenotypes, including laterality defects and neural tube dorsalization, can be explained by ciliary defects in the node and neural tube, respectively. However, as

reported for Mks1, Tctn1 is not essential for ciliogenesis in all tissues<sup>25</sup>. For example, anterior to the node, the notochord of *Tctn1*<sup>-/-</sup> embryos produces cilia, as does the early gut epithelium (Figure 1g and data not shown). Similarly, mesenchymal cells surrounding the neural tube possess acetylated tubulin (AcTub) containing cilia, as do limb bud mesenchymal cells (Figure 1h-i). Nevertheless, these cilia display markedly reduced levels of Arl13b (Figure 1h-i). Therefore, loss of Tctn1 has different effects in different tissues, with tissues such as the node and neural tube requiring Tctn1 for ciliogenesis, and tissues such as the perineural and limb bud mesenchyme requiring Tctn1 for ciliary localization of Arl13b.

The differential requirements for Tctn1 may reflect different ciliogenic mechanisms in the node and neural tube versus the mesenchyme. In support of this hypothesis, Ift20, a ciliogenic component of the intraflagellar transport complex B (IFT-B), localizes differently in neural tube and perineural mesenchyme cells (Figure S1c)<sup>26</sup>. Consistent with previous reports, Ift20 is Golgi-localized in mesenchymal cells, but not in the neural tube (Figure S1c)<sup>27</sup>. In contrast, Ift88, another IFT-B component, is present in both mesenchymal and neural cilia (Figure S1d). Thus, differential localization of ciliogenic proteins in mesenchymal and neural cells may signify different mechanisms of ciliogenesis, one of which is dependent on Tctn1.

To assess whether Tctn1 participates in ciliary function even where it is dispensable for ciliogenesis, we examined patterning of the limb bud, which contains cilia in Tctn1 mutants (Figure 1i). Shh specifies vertebrate digit number and identity by preventing cilium-dependent formation of Gli3 repressor (Gli3-R)<sup>28-29</sup>. Consequently, both increased Hh signaling or decreased ciliary function in the limb bud result in polydactyly<sup>2</sup>.

*Tctn1*<sup>-/-</sup> embryos developed an extra preaxial digit 1 on one or both hindlimbs (Figure 1j). Consistent with a role for Tctn1 in Hh signal transduction, *Shh* expression was unaffected in *Tctn1*<sup>-/-</sup> limb buds, but Shh-regulated genes, including *Fgf4*, *Bmp2*, *Gremlin* and *Hoxd11* were expanded anteriorly (Figure 1k)<sup>30</sup>. Similarly, two general Hh transcriptional targets, *Gli1* and *Ptch1*, were also expanded anteriorly in *Tctn1*<sup>-/-</sup> limb buds (Figure 1k). In contrast, expression of *Fgf8*, a Shh-independent gene, was unaltered, indicating that patterning, not formation, of the apical ectodermal ridge depends on Tctn1 (Figure 1k).

As shown previously for the neural tube, *Tctn1* was epistatic to *Shh* in limb bud patterning (Figure 1l)<sup>22</sup>. Compared to controls, *Tctn1*<sup>-/-</sup> embryos had markedly increased levels of full length Gli3 (Gli3-FL), suggesting that Gli3 processing is compromised (Figure 1m). These results indicate that, although Tctn1 is not required for ciliogenesis in the limb bud, it is required for cilium-dependent Hh signal transduction.

## Tctn1 is part of a ciliopathy-associated protein complex

To elucidate the role of Tctn1 in ciliogenesis, we generated NIH-3T3 cells stably expressing Tctn1 fused to a localization and affinity purification (LAP) tag<sup>31</sup>. These cells were ciliated and Tctn1-LAP was at the base of some cilia, although most Tctn1-LAP was retained in the endoplasmic reticulum (ER) (Figure 2a). To identify Tctn1-associated proteins, we isolated Tctn1-LAP by tandem affinity purification and analyzed copurifying interactors by mass

spectrometry. Using a cutoff of three unique peptides, we identified 154 proteins specifically in the Tctn1-LAP purification (Table S1). Among the proteins with the highest number of mass spectra, a measure of the amount of copurified protein, were the products of several genes associated with MKS, JBTS and other ciliopathies, including Mks1, Cep290, Cc2d2a, Tctn2 and B9d1 (Figure 2b)<sup>5,9–11,32</sup>. The two strongest Tctn1 interactors were Tctn2 and Tctn3, indicating that the three Tectonics are part of the same complex. None of these proteins were detected in a control purification from LAP-only expressing NIH-3T3 cells (Table S1).

Proteins represented by fewer mass spectra included several ER chaperones, possibly reflecting ER processing of Tctn1-LAP (Table S1). However, as Tctn1 colocalizes with ciliopathy proteins at the ciliary transition zone (shown below), it is likely that some of these interactions reflect ER retention of overexpressed Tctn1.

To confirm the interactions of Tctn1 with ciliopathy proteins, we performed coimmunoprecipitation assays using tagged proteins expressed in COS1 cells. Tctn1 interacted with Tctn2, Tctn3, Mks1, Cc2d2a and B9d1 (Figure 2c). Other ciliary or basal body proteins, including Smo, Rab8a and Rab11a, did not interact with Tctn1 (Figure 2c)<sup>4</sup>. Intriguingly, Tctn1 and Cep290 did not reproducibly interact by coimmunoprecipitation in COS1 cells, possibly indicating that the interaction of Tctn1 with Cep290 is compromised by tagging Cep290, or depends on immunoprecipitation conditions or cell type.

As our proteomic analysis identified five of the eight known MKS proteins, we tested whether Tctn1 associates with the other three: Tmem67, Tmem216 and Rpgrip11<sup>9–10</sup>. In transfected COS1 cells, Tctn1 interacted with Tmem67 and Tmem216, but not Rpgrip11 (Figure 2c-d). Thus, Tctn1 interacts with Mks1, Cc2d2a, B9d1, Tctn2, Tctn3 and, under some conditions, Tmem216, Tmem67 and Cep290. In addition, using antibodies against endogenous proteins, we found that Tctn2 interacts with Mks1 and Tctn3 in ciliated hTERT-RPE1 cells (Figure S2).

To investigate the size of the Tectonic ciliopathy complex, we subjected Tctn1-LAP purified from stably expressing NIH-3T3 cells to gel filtration chromatography (Figure 2e). We analyzed the fractions for protein concentration and the presence of Tctn1, Tctn2, Mks1, Cc2d2a and Cep290. Interestingly, these proteins co-eluted in fractions 15–19, corresponding to a molecular weight between 0.7 and 2 MDa, suggesting that they comprise one or a set of related large complexes.

### **Localization of Mks1 and Tmem67 to the ciliary transition zone depends upon Tctn1**

To investigate the function of Tectonic and MKS proteins in ciliogenesis, we examined their subcellular localization. The specificity of antibodies against Tctn1–3, Tmem67 and Cc2d2a was confirmed using siRNA-treated cells or cells harboring null alleles for these genes (Figures S2a, S3a-c). In hTERT-RPE1 cells, Tctn1 localized to the transition zone, between the ciliary axoneme and basal body (Figure 3a, S3d). The Tctn1 interactors Tctn2, Tctn3, Mks1, Tmem67, Cep290, Cc2d2a and B9d1 also localized to the transition zone (Figure 3a, S3d). In addition, Nphp4, not detected as a Tctn1 interactor, localized to the transition zone (Figure 3a, S3d). Some of these proteins also localized to the basal body (B9d1), cilium

proper (Tctn2, Tctn3, Tmem67), or centriolar satellites (Cep290). Tmem216 occasionally localized to the transition zone, but more typically localized to the basal body or axoneme. Rpgrip11, the only MKS protein that did not biochemically interact with Tctn1, localized to the basal body, similar to BBSome component Bbs5.

To understand how Tctn1 contributes to transition zone function, we examined whether Tctn1 controls the organization of the transition zone (Figure 3b, S3e-g). Several transition zone proteins, including Nphp1, Nphp4, RP2 and Septin2, localized independently of Tctn1<sup>5,8,33-34</sup>. The same was true of Bbs5, Ift88 and Ift139, components of the BBSome, IFT-B and IFT-A ciliary protein complexes, respectively, and of Rpgrip11, which localized to the transition zone of MEFs. Tmem216 localization to the basal body and, variably, to the transition zone was also unaffected. Similarly, Cc2d2a was at the transition zone of *Tctn1*<sup>-/-</sup> MEFs, indicating that at least some Tctn1 interactors localize to the transition zone independently of Tctn1. In contrast, *Tctn1*<sup>-/-</sup> MEFs exhibited decreased Mks1 and Tmem67 localization to the transition zone (Figure 3b-c, S3e). These results reveal that Tctn1 is required for transition zone localization of a subset of interacting proteins.

### Tctn1 interactors Tctn2, Cc2d2a and Tmem67 also promote tissue-specific ciliogenesis

To assess Tectonic complex function, we analyzed mouse *Tctn2*, *Cc2d2a* and *Tmem67* mutants. Mice homozygous for the *Tctn2* mutant allele displayed phenotypes closely resembling those of *Tctn1* mutants<sup>5</sup>. Like *Tctn1*<sup>-/-</sup> embryos, *Tctn2*<sup>-/-</sup> embryos lacked nodal cilia, as determined by immunostaining and SEM (Figure 4a-b). Cilia in *Tctn2*<sup>-/-</sup> neural tubes were scarce, morphologically defective, and failed to elongate axonemes (Figures 4c-d, S4). Also similar to *Tctn1* mutants, basal bodies docked to the plasma membrane in *Tctn2*<sup>-/-</sup> neural epithelium (Figures 4d, S4b). In the limb bud mesenchyme, cilia numbers were reduced, yet the remaining cilia appeared normal by AcTub and  $\gamma$ -tubulin staining (Figure 4e). In contrast, no Arl13b ciliary staining was seen in *Tctn2*<sup>-/-</sup> perineural mesenchyme, suggesting that, as in *Tctn1*<sup>-/-</sup> mutants, *Tctn2*<sup>-/-</sup> cilia lack Arl13b (Figure 4f). These data suggest that Tctn1 and Tctn2 share a common function, with both affecting ciliogenesis in a tissue-specific manner.

We also generated mice mutant for *Cc2d2a* (Figure S5a). *Cc2d2a*<sup>-/-</sup> embryos exhibit randomized left-right axes, holoprosencephaly, microphthalmia, and a variably expressive curved body axis, phenotypes also exhibited by *Tctn1* and *Tctn2* mutants (Figure 5a and data not shown)<sup>22</sup>. *Cc2d2a*<sup>-/-</sup> embryos also have cilia defects, exemplified by the absence of Arl13b staining in the neural tube and surrounding mesenchyme (Figure 5b-c). Furthermore, like *Tctn1*<sup>-/-</sup> MEFs, *Cc2d2a*<sup>-/-</sup> MEFs can generate cilia (Figure 5d). Thus, Cc2d2a shares tissue-specific ciliogenic functions with Tctn1 and Tctn2.

Finally, we analyzed mice homozygous for a targeted allele of *Tmem67* (Figures 5e-g, S5b-d). Unlike *Tctn1*, *Tctn2* or *Cc2d2a* mutants, *Tmem67*<sup>-/-</sup> mice survived to birth with no overt morphological abnormalities. However, these mice died soon after birth (Figure S5c-d). These results are similar to those of *bpck* mutants, which harbor a large genomic deletion including *Tmem67* and five other genes<sup>35</sup>. *bpck* mutants develop kidney cysts, and cilia of *bpck* mutant kidney tubules are dysmorphic and vary in length<sup>35</sup>.

We examined the kidneys of E18.5 *Tmem67*<sup>-/-</sup> embryos (Figure 5e-f). Consistent with the *bpck* phenotype, *Tmem67*<sup>-/-</sup> embryonic kidneys develop cysts (Figure 5e), and kidney tubules have fewer cilia than controls (Figure 5f). *Tmem67* siRNA-treated IMCD3 kidney cells also display ciliogenesis defects<sup>36</sup>. In contrast, *Tmem67*<sup>-/-</sup> MEFs were not defective in ciliogenesis (Figure 5g). Hence, *Tmem67* also has tissue-specific roles in ciliogenesis, although the ciliogenic defects are milder than those of *Tctn1*, *Tctn2* or *Cc2d2a* mutants.

Given that *Tmem67* and *Tctn1* mutants display distinct phenotypes, we generated *Tmem67*<sup>-/-</sup> *Tctn1*<sup>-/-</sup> double mutant embryos to examine the genetic relationship between both genes. Double mutant embryos were indistinguishable from *Tctn1*<sup>-/-</sup> single mutants (Figure 5h). As compared to *Tctn1*, *Tctn2*, and *Cc2d2a* mutants, the weaker phenotypes of *Tmem67* null mutants suggest that *Tmem67* has an ancillary role in promoting the ciliogenic functions of the core *Tctn1*, *Tctn2*, and *Cc2d2a* complex.

### The Tectonic ciliopathy complex controls ciliary membrane protein localization

All *Tctn* genes encode signal peptides and are thus predicted to be translated at the ER. Consistently, *Tctn1* undergoes N-glycosylation and, when overexpressed, is seen at the ER (Figures 2a, S6a). *Tctn2* and 3, but not *Tctn1*, have predicted transmembrane helices in their carboxy-termini. Despite the absence of a transmembrane domain, *Tctn1* is not secreted and functions cell autonomously (Figure S6b-c and data not shown).

Given the association of Tectonics with membranes and the transition zone, we hypothesized that *Tctn1* regulates ciliary membrane composition. We examined the localization of GFP-tagged SSTR3, a G protein-coupled receptor that can localize to cilia<sup>16</sup>. This protein localized to cilia equally in wild type and *Tctn1*<sup>-/-</sup> MEFs (Figure S6d).

Adenylyl cyclase III (AC3) is another multipass transmembrane protein that localizes to primary cilia of adult mouse brains<sup>37</sup>. AC3 also localizes to cilia in wild type MEFs and E14.5 embryos, but not in *Tctn1*<sup>-/-</sup> MEFs or embryos (Figure 6). We examined whether *Tctn1* interacting proteins are similarly required for ciliary membrane protein localization. Strikingly, MEFs lacking *Tctn2*, *Cc2d2a* or *Tmem67* lacked AC3 in their cilia (Figure 6). Thus, the Tectonic complex is required for the ciliary localization of AC3.

*Pkd2*, the product of a gene mutated in autosomal dominant polycystic kidney disease, is another ciliary transmembrane protein<sup>9-10,14</sup>. *Pkd2* localizes to cilia in some wild type MEFs but, like AC3, its ciliary localization is abrogated in *Tctn1*<sup>-/-</sup>, *Tctn2*<sup>-/-</sup> and *Cc2d2a*<sup>-/-</sup> MEFs, and in *Tctn1*<sup>-/-</sup> E14.5 mesenchyme (Figure 6). *Pkd2* also localizes to cilia in some wild type E18.5 kidney tubules, and this was unchanged in *Tmem67*<sup>-/-</sup> kidneys, indicating that *Tmem67*, unlike other complex components, is not required for ciliary localization of *Pkd2* (Figure 6f)<sup>38</sup>.

*Smo* is a seven transmembrane protein that moves to cilia in response to Hh pathway activation<sup>20</sup>. *Smo* displayed reduced ciliary localization in *Tctn1*<sup>-/-</sup> and *Tctn2*<sup>-/-</sup> MEFs treated with the Hh pathway agonist SAG, an effect that was even stronger in *Cc2d2a*<sup>-/-</sup> MEFs (Figure 6)<sup>39</sup>. In contrast, SAG-treated *Tmem67*<sup>-/-</sup> MEFs displayed normal levels of ciliary *Smo*, again consistent with an ancillary role for *Tmem67* in the Tectonic complex.

*Tctn1*<sup>-/-</sup>, *Tctn2*<sup>-/-</sup> and *Cc2d2a*<sup>-/-</sup> MEFs also displayed dramatically reduced levels of ciliary Arl13b, whereas *Tmem67*<sup>-/-</sup> MEFs had a more modest reduction (Figure 6). Although Arl13b is not an integral membrane protein, it is membrane-associated via palmitoylation<sup>24</sup>. Consistent with a role for Tctn1 in controlling ciliary protein composition, transfection of *Tctn1*<sup>-/-</sup> MEFs with myc- or LAP-tagged Tctn1 rescued ciliary localization of Arl13b and AC3 (Figure S6e-f and data not shown).

Taken together, these results suggest that the Tectonic ciliopathy complex acts at the transition zone to control ciliary membrane protein composition.

### A human *TCTN1* mutation is a cause of JBTS

Given the connections between Tctn1 and recognized ciliopathy proteins, we examined whether human *TCTN1* gene mutations also cause ciliopathies. We used homozygosity mapping in consanguineous kindreds with consecutive exon sequencing to test whether *TCTN1* mutations are associated with ciliopathies<sup>41</sup>.

In kindred A2090 from Bangladesh, the parents of two sisters with JBTS were first degree cousins. In both sisters (II-1 and II-2), brain MRI revealed cerebellar vermis hypoplasia and the “molar tooth sign”, the characteristic radiographic feature of JBTS. Sibling II-1 also had bilateral frontotemporal pachygyria, a coarsening of the cerebral gyri. Ophthalmologic assessment and renal ultrasounds of siblings II-1 and II-2 were normal at ages 7 and 4 yrs, respectively.

Homozygosity mapping of this kindred identified nine segments of homozygosity by descent, representing candidate regions for a recessive disease-causing mutation (Figure 7a)<sup>41</sup>. Because none of these segments coincided with known ciliopathy loci, we hypothesized that JBTS in family A2090 is caused by a recessive mutation in an unrecognized ciliopathy gene. *TCTN1* mapped to a homozygous candidate region on chromosome 12 (Figure 7a). Direct Sanger sequencing of all *TCTN1* exons revealed a homozygous obligatory splice-acceptor mutation (IVS1-2a>g) in both affected siblings of family A2090 (Figure 7b). This mutation, predicted to disrupt domains of the TCTN1 protein required for its function (Figure S7), was absent from 96 healthy control individuals and from the 1,000 Genomes Project, thus confirming *TCTN1* mutation as a new cause of JBTS. Investigation of four families homozygous at the *TCTN1* locus and 48 families with JBTS revealed no additional mutations, suggesting that *TCTN1* mutations are a rare cause of JBTS.

## DISCUSSION

By combining developmental, genetic, and biochemical analyses, we have identified a complex containing Tctn1, Tctn3 and seven MKS proteins (Mks1, Tmem216, Tmem67, Cep290, Cc2d2a, B9d1 and Tctn2). This complex localizes to the ciliary transition zone, where it regulates ciliogenesis and ciliary membrane composition in a tissue-dependent manner. Together with the MKS-like phenotypes exhibited by mouse Tectonic mutants, our data suggest transition zone dysfunction is the cell biological defect underlying human MKS.



Tctn1 modulates Hh signaling in the mouse neural tube<sup>22</sup>. As both Gli activator and repressor activity depend on cilia, the role of Tctn1 in neural tube patterning is likely due to its requirement in neural ciliogenesis<sup>28–29</sup>. Tctn1 also participates in Hh signaling in the limb bud. However, Tctn1 is not required for limb ciliogenesis, but promotes ciliary translocation of Arl13b and Smo, both involved in Hh signaling<sup>20,23</sup>. Therefore, the role of Tctn1 in regulating ciliary membrane composition may underlie its function in limb patterning.

The mechanisms underlying tissue specificity of Tectonic complex function remain unclear. Cilia from different tissues possess different functions and compositions, perhaps reflecting different ciliogenic mechanisms. In support of this hypothesis, the ciliogenic protein Ift20 localizes to the Golgi in mesenchymal but not neural cells. Given that the transition zone is formed early during ciliogenesis, the transition zone may regulate the entrance of IFT particles into the nascent axoneme in some cell types<sup>6</sup>.

Cep290 was identified as a Tctn1 interactor by mass spectrometry and chromatography, but not coimmunoprecipitation. In contrast, Tmem67 and Tmem216 were not detected by mass spectrometry, but did coimmunoprecipitate with Tctn1. Thus, Cep290, Tmem67 and Tmem216 may be substoichiometric or peripheral components of the Tectonic complex. Besides ciliopathy proteins, our mass spectrometric analysis identified many additional potential Tctn1 interactors. Although most of these were considerably less abundant in the Tctn1 purification than the ciliopathy proteins, they may still participate in Tectonic complex function.

We identified a *TCTN1* mutation causing JBTS, an MKS-related ciliopathy. *TCTN2* mutations also lead to MKS and JBTS, underscoring the connection between *TCTN* genes and human ciliopathies<sup>5,11</sup>. Moreover, mutations in *ARL13B*, whose ciliary localization depends on Tectonics, similarly cause JBTS<sup>42</sup>. Apart from MKS, *TMEM216*, *TMEM67* and *CC2D2A* are associated with JBTS and COACH syndromes<sup>9–10</sup>. How do these genes display such a high degree of allelism? We propose that different degrees of complex dysfunction manifest as different syndromes, with severe loss of function causing MKS, and progressively less severe impairment causing COACH and JBTS (Figure 7c). Consistent with this model, mouse *Tctn1*, *Tctn2*, *Cc2d2a* and *Mks1* null mutants display phenotypes resembling human MKS, whereas *Tmem67* mutants have a less severe phenotype, suggesting partial loss of Tectonic complex function<sup>25</sup>.

Like *Tctn* mutants, *Rpgrip11* mutant mice display MKS-like phenotypes<sup>43</sup>. However, *Rpgrip11* does not interact with Tctn1, and instead forms a transition zone complex with *Nphp1* and *Nphp4*<sup>5</sup>. This NPHP complex functions together with the Tectonic complex, as the nematode orthologs of *Nphp* genes genetically interact with components of the Tectonic complex<sup>6</sup>. Moreover, *C. elegans* *Rpgrip11* regulates transition zone localization of both complexes<sup>6</sup>. In contrast, mammalian Tctn1 is required for proper localization of some Tectonic complex members, but not for the NPHP complex. Thus, transition zone integrity depends upon both complexes operating in a partially redundant manner.

In contrast to the Tectonic complex, severe dysfunction of the NPHP complex may result in Senior-Løken syndrome (SLSN), characterized by NPHP with retinitis pigmentosa. Some ciliopathies may also result from abrogated activity of both the NPHP and Tectonic complexes, as exemplified by the minority of JBTS patients who also have NPHP and retinitis pigmentosa (Figure 7c)<sup>9–10</sup>. The phenotypic diversity caused by transition zone dysfunction may relate to whether mutations abrogate or spare ciliogenesis, in addition to disrupting ciliary membrane composition. The former may result in MKS, COACH or JBTS, while the latter may cause SLSN or NPHP.

In BBS, BBSome disruption also leads to ciliary composition defects, raising the question of how BBSome and Tectonic complexes are functionally connected<sup>16,18</sup>. Interestingly, AC3 entrance into cilia is BBSome-independent<sup>16,18</sup>, but Tectonic-dependent. Hence, the BBSome and Tectonic complexes may control ciliary localization of different membrane proteins. Moreover, BBSome subunits do not interact with Tctn1 and do not localize to the transition zone, indicating that BBSome and Tectonic complexes operate at different suborganellar locations<sup>16–17</sup>. The BBSome acts as a coat that traffics membrane proteins to the cilium, and is itself an IFT cargo, suggesting that BBSome-associated proteins enter the cilium aboard IFT trains<sup>16,44</sup>. If so, such trains need to pass the transition zone station, which might be the site of a crossing gate mediated by the Tectonic complex.

The transition zone is best known in *Chlamydomonas*, whose Cep290 ortholog controls flagellar protein content<sup>7,45</sup>. The similarity of *Chlamydomonas Cep290* and vertebrate Tectonic complex mutants suggests that the ciliary functions of the Tectonic complex are conserved deeply through evolution. Accordingly, *Tmem67* and *Cc2d2a* orthologs are found in all Tectonic-possessing eukaryotes for which genomic information exists, and these Tectonic complex components were likely to be possessed by the eukaryotic ancestor (Figure S8). Other transition zone components, such as *Cep290*, are not present in the genomes of many ciliated unicellular organisms, or even all bilaterians, suggesting that their roles in the complex are dispensable for some ciliary functions<sup>1</sup>.

In summary, we have identified a transition zone complex of MKS and JBTS proteins that regulates ciliogenesis and ciliary membrane composition. The identification of physical interactions and functional similarities between Tctn1 and other complex components suggests that the transition zone is compromised in human MKS and JBTS. In support of this conclusion, mutations in human *TCTN1* are a rare cause of JBTS.

## Supplementary Material

Refer to Web version on PubMed Central for supplementary material.

## Acknowledgments

The authors thank the IRM and Nikon Imaging Centers at UCSF. The *Servei Central de Suport a la Investigació Experimental* and Mario Soriano-Navarro assisted with EM. Members of the Reiter lab provided valuable discussions. Kathryn Anderson, David Beier, Joseph Gleeson, Colin Johnson, Hemant Khanna, Robert Molday, Kirk Mykytyn Gregory Pazour, Suzie Scales, James Sillibourne, and Stefan Somlo provided antibodies or plasmids. T.R.N. is supported by an NSF predoctoral grant and an NIGMS-IMSD grant (R25-GM56847). F.H. is an Investigator of the Howard Hughes Medical Institute, a Doris Duke Distinguished Clinical Scientist and a Frederick G. L. Huetwell Professor. This work was funded by grants from the National Institutes of Health to F.H.

(DK1069274, DK1068306, RC4-K090917) and to J.F.Reiter (AR054396), and from the March of Dimes, the Burroughs Wellcome Fund, the Packard Foundation, and the Sandler Family Supporting Foundation to J.F.Reiter.

## References

1. Hodges ME, Scheumann N, Wickstead B, Langdale JA, Gull K. Reconstructing the evolutionary history of the centriole from protein components. *J Cell Sci.* 2010; 123:407–413.
2. Goetz SC, Anderson KV. The primary cilium: a signalling centre during vertebrate development. *Nat Rev Genet.* 2010; 11:331–344. [PubMed: 20395968]
3. Sorokin S. Centrioles and the formation of rudimentary cilia by fibroblasts and smooth muscle cells. *J Cell Biol.* 1962; 15:363–377. [PubMed: 13978319]
4. Nachury MV, Seeley ES, Jin H. Trafficking to the Ciliary Membrane: How to Get Across the Periciliary Diffusion Barrier? *Annu Rev Cell Dev Biol.* 2010; 26:59–87. [PubMed: 19575670]
5. Sang L, et al. Mapping the NPHP-JBTS-MKS Protein Network Reveals Ciliopathy Disease Genes and Pathways. *Cell.* 2011; 145:513–528. [PubMed: 21565611]
6. Williams CL, et al. MKS and NPHP modules cooperate to establish basal body/transition zone membrane associations and ciliary gate function during ciliogenesis. *J Cell Biol.* 2011; 192:1023–1041. [PubMed: 21422230]
7. Craig B, et al. CEP290 tethers flagellar transition zone microtubules to the membrane and regulates flagellar protein content. *J Cell Biol.* 2010; 190:927–940. [PubMed: 20819941]
8. Hu Q, et al. A septin diffusion barrier at the base of the primary cilium maintains ciliary membrane protein distribution. *Science.* 2010; 329:436–439. [PubMed: 20558667]
9. Tobin JL, Beales PL. The nonmotile ciliopathies. *Genet Med.* 2009; 11:386–402. [PubMed: 19421068]
10. Hildebrandt F, Benzing T, Katsanis N. Ciliopathies. *N Engl J Med.* 2011; 364:1533–1543. [PubMed: 21506742]
11. Shaheen R, et al. A TCTN2 mutation defines a novel meckel gruber syndrome locus. *Hum Mutat.* Apr 1.2011 Epub ahead of print.
12. Leitch CC, et al. Hypomorphic mutations in syndromic encephalocele genes are associated with Bardet-Biedl syndrome. *Nat Genet.* 2008; 40:443–448. [PubMed: 18327255]
13. Khanna H, et al. A common allele in RPGRIP1L is a modifier of retinal degeneration in ciliopathies. *Nat Genet.* 2009; 41:739–745. [PubMed: 19430481]
14. Geng L, et al. Polycystin-2 traffics to cilia independently of polycystin-1 by using an N-terminal RVxP motif. *J Cell Sci.* 2006; 119:1383–1395. [PubMed: 16537653]
15. Mazelova J, et al. Ciliary targeting motif VxPx directs assembly of a trafficking module through Arf4. *EMBO J.* 2009; 28:183–192. [PubMed: 19153612]
16. Jin H, et al. The conserved Bardet-Biedl syndrome proteins assemble a coat that traffics membrane proteins to cilia. *Cell.* 2010; 141:1208–1219. [PubMed: 20603001]
17. Nachury MV, et al. A core complex of BBS proteins cooperates with the GTPase Rab8 to promote ciliary membrane biogenesis. *Cell.* 2007; 129:1201–1213. [PubMed: 17574030]
18. Berbari NF, Lewis JS, Bishop GA, Askwith CC, Mykytyn K. Bardet-Biedl syndrome proteins are required for the localization of G protein-coupled receptors to primary cilia. *Proc Natl Acad Sci U S A.* 2008; 105:4242–4246. [PubMed: 18334641]
19. Mykytyn K, et al. Bardet-Biedl syndrome type 4 (BBS4)-null mice implicate Bbs4 in flagella formation but not global cilia assembly. *Proc Natl Acad Sci U S A.* 2004; 101:8664–8669. [PubMed: 15173597]
20. Corbit KC, et al. Vertebrate Smoothed functions at the primary cilium. *Nature.* 2005; 437:1018–1021. [PubMed: 16136078]
21. Boehlke C, et al. Primary cilia regulate mTORC1 activity and cell size through Lkb1. *Nat Cell Biol.* 2010; 12:1115–1122. [PubMed: 20972424]
22. Reiter JF, Skarnes WC. Tectonic, a novel regulator of the Hedgehog pathway required for both activation and inhibition. *Genes Dev.* 2006; 20:22–27. [PubMed: 16357211]

23. Caspary T, Larkins CE, Anderson KV. The graded response to Sonic Hedgehog depends on cilia architecture. *Dev Cell*. 2007; 12:767–778. [PubMed: 17488627]
24. Cevik S, et al. Joubert syndrome Arl13b functions at ciliary membranes and stabilizes protein transport in *Caenorhabditis elegans*. *J Cell Biol*. 2010; 188:953–969. [PubMed: 20231383]
25. Weatherbee SD, Niswander LA, Anderson KV. A mouse model for Meckel syndrome reveals Mks1 is required for ciliogenesis and Hedgehog signaling. *Hum Mol Genet*. 2009; 18:4565–4575. [PubMed: 19776033]
26. Jonassen JA, San Agustin J, Follit JA, Pazour GJ. Deletion of IFT20 in the mouse kidney causes misorientation of the mitotic spindle and cystic kidney disease. *J Cell Biol*. 2008; 183:377–384. [PubMed: 18981227]
27. Follit JA, San Agustin JT, Xu F, Jonassen JA, Samtani R, Lo CW, Pazour GJ. Golgin GMAP210/TRIP11 anchors IFT20 to the Golgi complex. *PLoS Genet*. 2008; 4:e1000315. [PubMed: 19112494]
28. Huangfu D, et al. Hedgehog signalling in the mouse requires intraflagellar transport proteins. *Nature*. 2003; 426:83–87. [PubMed: 14603322]
29. Liu A, Wang B, Niswander LA. Mouse intraflagellar transport proteins regulate both the activator and repressor functions of Gli transcription factors. *Development*. 2005; 132:3103–3111. [PubMed: 15930098]
30. Bénazet JD, Zeller R. Vertebrate limb development: moving from classical morphogen gradients to an integrated 4-dimensional patterning system. *Cold Spring Harb Perspect Biol*. 2009; 1:a001339. [PubMed: 20066096]
31. Torres JZ, Miller JJ, Jackson PK. High-throughput generation of tagged stable cell lines for proteomic analysis. *Proteomics*. 2009; 9:2888–2891. [PubMed: 19405035]
32. Hopp K, et al. B9D1 is revealed as a novel Meckel syndrome (MKS) gene by targeted exon-enriched next-generation sequencing and deletion analysis. *Hum Mol Genet*. Apr 27.2011 Epub ahead of print.
33. Won J, et al. NPHP4 is necessary for normal photoreceptor ribbon synapse maintenance and outer segment formation, and for sperm development. *Hum Mol Genet*. 2011; 20:482–96. [PubMed: 21078623]
34. Holopainen JM, et al. Interaction and Localization of the Retinitis Pigmentosa Protein RP2 and NSF in Retinal Photoreceptor Cells. *Biochemistry*. 2010; 49:7439–7447. [PubMed: 20669900]
35. Cook SA, et al. A mouse model for Meckel syndrome type 3. *J Am Soc Nephrol*. 2009; 20:753–764. [PubMed: 19211713]
36. Dawe HR, et al. The Meckel-Gruber Syndrome proteins MKS1 and meckelin interact and are required for primary cilium formation. *Hum Mol Genet*. 2007; 16:173–186. [PubMed: 17185389]
37. Bishop GA, Berbari NF, Lewis J, Mykytyn K. Type III adenylyl cyclase localizes to primary cilia throughout the adult mouse brain. *J Comp Neurol*. 2007; 505:562–571. [PubMed: 17924533]
38. Pazour GJ, San Agustin JT, Follit JA, Rosenbaum JL, Witman GB. Polycystin-2 localizes to kidney cilia and the ciliary level is elevated in *orpk* mice with polycystic kidney disease. *Curr Biol*. 2002; 12:R378–R380. [PubMed: 12062067]
39. Chen JK, Taipale J, Young KE, Maiti T, Beachy PA. Small molecule modulation of Smoothened activity. *Proc Natl Acad Sci U S A*. 2002; 99:14071–14076. [PubMed: 12391318]
40. Attanasio M, et al. Loss of GLIS2 causes nephronophthisis in humans and mice by increased apoptosis and fibrosis. *Nat Genet*. 2007; 39:1018–1024. [PubMed: 17618285]
41. Hildebrandt F, et al. A systematic approach to mapping recessive disease genes in individuals from outbred populations. *PLoS Genet*. 2009; 5:e1000353. [PubMed: 19165332]
42. Cantagrel V, et al. Mutations in the cilia gene ARL13B lead to the classical form of Joubert syndrome. *Am J Hum Genet*. 2008; 83:170–179. [PubMed: 18674751]
43. Vierkotten J, Dildrop R, Peters T, Wang B, Rütger U. Ftm is a novel basal body protein of cilia involved in Shh signalling. *Development*. 2007; 134:2569–2577. [PubMed: 17553904]
44. Lehtreck KF, et al. The *Chlamydomonas reinhardtii* BBSome is an IFT cargo required for export of specific signaling proteins from flagella. *J Cell Biol*. 2009; 187:1117–1132. [PubMed: 20038682]

45. Geimer S, Melkonian M. The ultrastructure of the *Chlamydomonas reinhardtii* basal apparatus: identification of an early marker of radial asymmetry inherent in the basal body. *J Cell Sci.* 2004; 117:2663–2674. [PubMed: 15138287]
46. Nagy, A.; Gertsenstein, M.; Vintersten, K.; Behringer, R. *Manipulating the Mouse Embryo: A Laboratory Manual.* 3. Cold Spring Harbor Lab Press; Cold Spring Harbor, New York, USA: 2002.
47. Kruglyak L, Daly MJ. Linkage thresholds for two-stage genome scans. *Am J Hum Genet.* 1998; 62:994–997. [PubMed: 9529350]
48. Strauch K, et al. Parametric and nonparametric multipoint linkage analysis with imprinting and two-locus-trait models: application to mite sensitization. *Am J Hum Genet.* 2000; 66:1945–1957. [PubMed: 10796874]
49. Gudbjartsson DF, Jonasson K, Frigge ML, Kong A. Allegro, a new computer program for multipoint linkage analysis. *Nat Genet.* 2000; 25:12–13. [PubMed: 10802644]
50. Otto EA, et al. Candidate exome capture identifies mutation of *SDCCAG8* as the cause of a retinal-renal ciliopathy. *Nat Genet.* 2010; 42:840–850. [PubMed: 20835237]

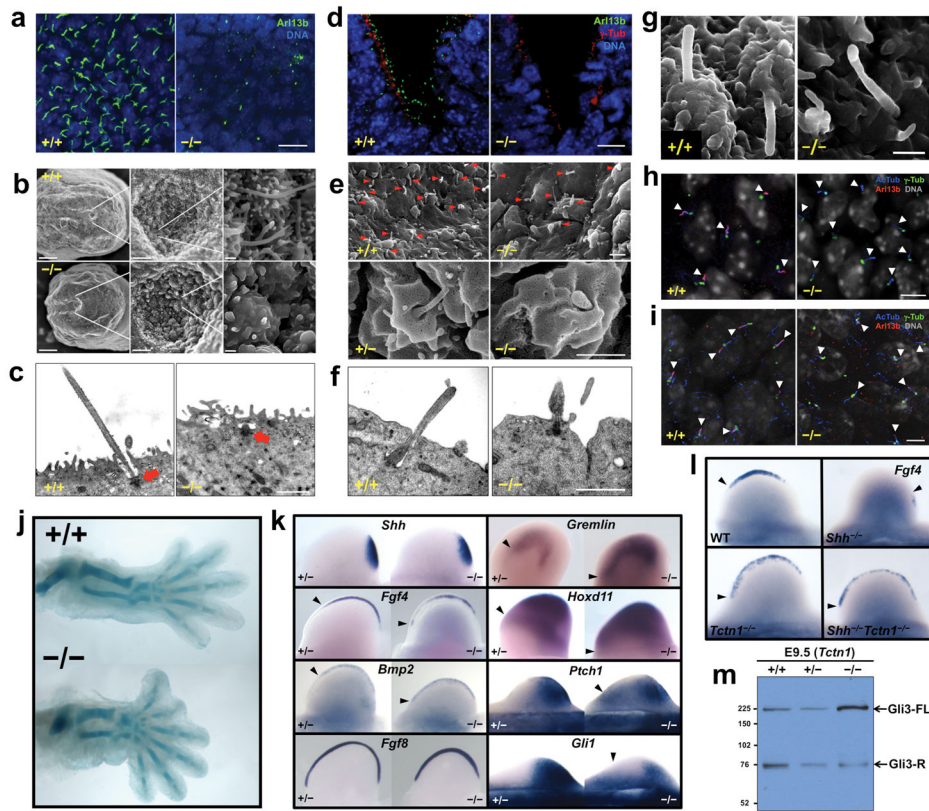


**Figure 1. *Tctn1* is required for ciliogenesis in a tissue-dependent manner**

(a) Wild type and *Tctn1*<sup>-/-</sup> E8.5 nodes stained for Arl13b (green) and DNA (DAPI, blue). Scale bar 10 $\mu$ m. (b) SEM of wild type and *Tctn1*<sup>-/-</sup> E8.0 nodes. Scale bars are 50 $\mu$ m, 5 $\mu$ m and 0.5 $\mu$ m in left, middle and right panels, respectively. (c) TEM of wild type and *Tctn1*<sup>-/-</sup> E8.5 nodes. Arrows indicate basal bodies. Scale bar 1 $\mu$ m. (d) Wild type and *Tctn1*<sup>-/-</sup> E10.5 ventral neural tube stained for Arl13b (green),  $\gamma$ -tubulin (red), and DNA (DAPI, blue). Scale bar 10 $\mu$ m. (e) SEM of wild type and *Tctn1*<sup>-/-</sup> E9.5 neural tubes. Arrowheads indicate cilia. Scale bars 1 $\mu$ m. (f) TEM of wild type and *Tctn1*<sup>-/-</sup> E9.5 neural tubes. Scale bar 1 $\mu$ m. (g) SEM of notochord cilia from wild type and *Tctn1*<sup>-/-</sup> E8.0 embryos. Scale bar 1 $\mu$ m. (h) E10.5 perineural mesenchyme sections were stained for AcTub (blue), Arl13b (red),  $\gamma$ -tubulin (green), and DNA (grey). Arl13b localization to *Tctn1*<sup>-/-</sup> cilia is reduced. Arrowheads indicate cilia. Scale bar 5 $\mu$ m. (i) E11.5 hindlimb bud mesenchyme sections were stained as in (h). Arl13b is also reduced in *Tctn1*<sup>-/-</sup> cilia. Arrowheads indicate cilia. Scale bar 5 $\mu$ m. (j) Alcian blue staining of wild type and *Tctn1*<sup>-/-</sup> E14.5 hindlimb cartilage. (k) In situ hybridization of E10.5 or E11.5 hindlimb buds for expression of the indicated genes. (l) In situ hybridization of E10.5 hindlimb buds for *Fgf4* expression reveals that *Tctn1* is epistatic to *Shh*. (m) Immunoblot of E9.5 wild type, *Tctn1*<sup>+/-</sup> and *Tctn1*<sup>-/-</sup> embryo extracts with Gli3 antibodies.

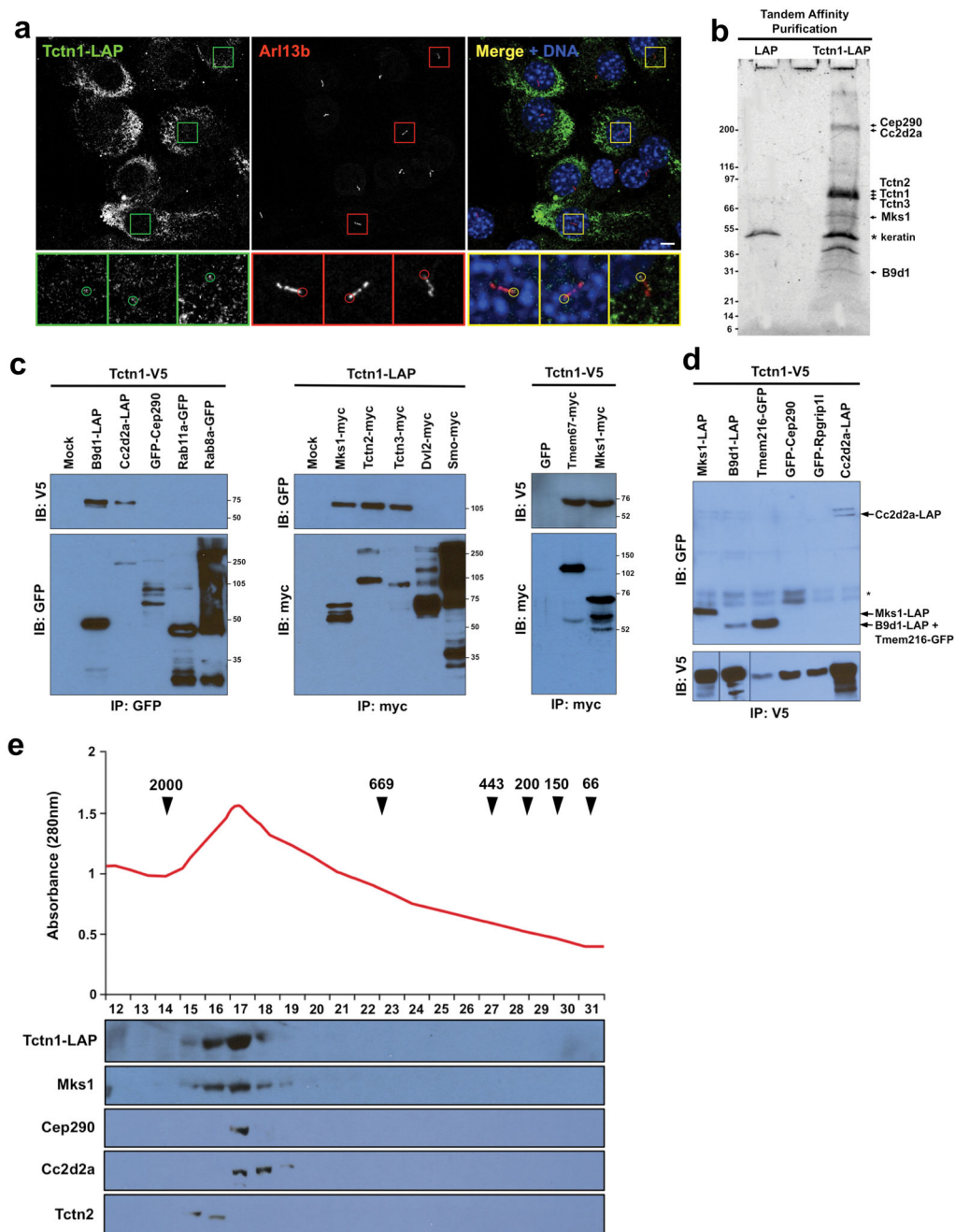


### Figure 2. Tctn1 interacts with ciliopathy proteins

(a) NIH-3T3 cells stably expressing Tctn1-LAP were stained for GFP, part of the LAP tag, and the ciliary marker Arl13b. Tctn1-LAP accumulates at the endoplasmic reticulum, and some Tctn1-LAP is seen at the base of some cilia (insets, 3X magnification of indicated regions). Scale bar 5  $\mu$ m. (b) Tctn1-LAP-associated proteins were purified from stable NIH-3T3 cells and separated by SDS-PAGE. SYPRO ruby staining of the gel revealed several major bands, whose identities were elucidated by mass spectrometry and are indicated on the right (a complete list of interactors is found in Table S1). The sizes of molecular weight markers appear on the left. A control purification is also shown. (c)

Immunoblot analysis of immunoprecipitates from lysates of COS1 cells transfected with constructs expressing tagged proteins as labeled at top demonstrated that Mks1, Tctn2, Tctn3, B9d1, Cc2d2a and Tmem67 can immunoprecipitate Tctn1. Size markers in kDa are shown on the right of each panel. **(d)** Reciprocal immunoprecipitation indicated that Tctn1-V5 can associate with tagged coexpressed Mks1, Tmem216, B9d1 and Cc2d2a. The locations of these proteins are indicated on the right. The asterisk indicates a pair of non-specific bands. **(e)** Tctn1-LAP was purified from NIH-3T3 cells and analyzed by gel filtration chromatography. The eluted fractions were analyzed for total protein amount (top) and by immunoblot for the indicated proteins. Arrowheads indicate the positions of molecular weight markers, in kDa.

Author Manuscript

Author Manuscript

Author Manuscript

Author Manuscript



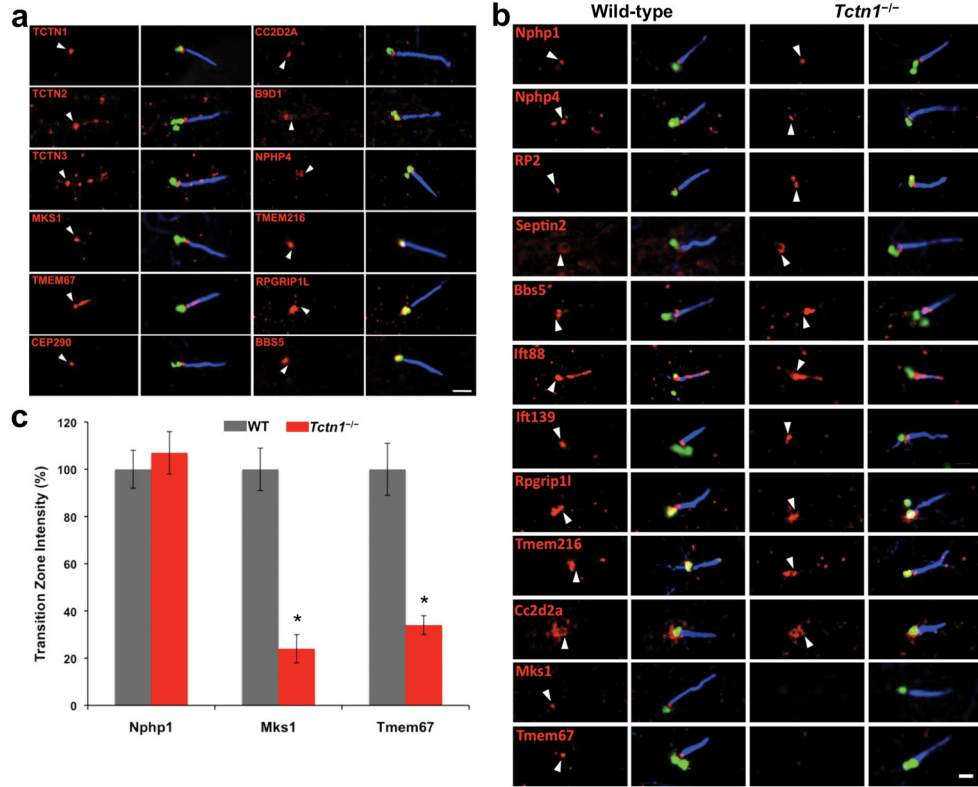


**Figure 3. Tctn1 and its interactors localize to the ciliary transition zone**  
**(a)** hTERT-RPE1 cells were stained for AcTub (blue), the basal body component  $\gamma$ -tubulin (or Ninein in the Cc2d2a panel) (green) and the indicated proteins (red). White arrowheads indicate the position of the transition zone. Note that Tctn1 and its interactors (Tctn2, Tctn3, Mks1, Tmem67, Cep290, Cc2d2a and B9d1) are present at the transition zone, although in some cases not exclusively. Scale bar 1 $\mu$ m. **(b)** MEFs from wild type and *Tctn1*<sup>-/-</sup> embryos were stained as above, except for Septin2 where detyrosinated tubulin, rather than AcTub, is shown in blue. The Tctn1 interactors Mks1, Tmem67 and Cc2d2a localize to the transition zone of wild type MEFs, but Mks1 and Tmem67 fail to localize to the transition zone of *Tctn1*<sup>-/-</sup> MEFs. Scale bar 1 $\mu$ m. **(c)** The intensity of transition zone staining in wild type and *Tctn1*<sup>-/-</sup> MEFs was quantified for Nphp1, Mks1 and Tmem67. Data are shown as mean  $\pm$  SEM. Asterisks denote statistical significance according to unpaired Student's t-tests (\* = p<0.01).

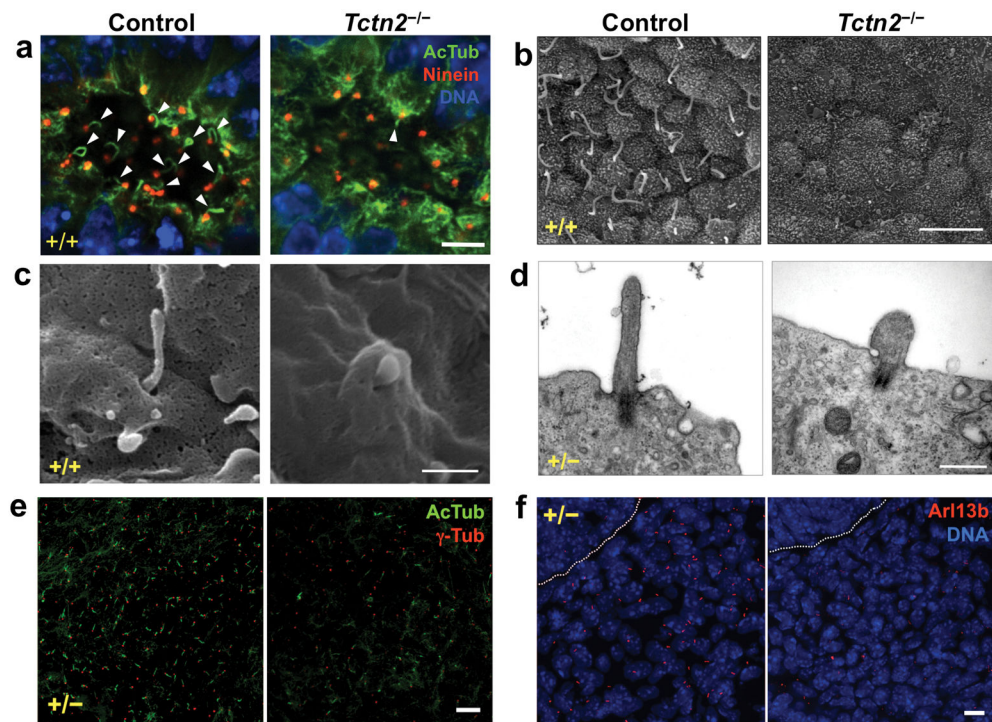


**Figure 4. *Tctn2*, like *Tctn1*, is essential for ciliogenesis in a tissue dependent manner**  
**(a)** Wild type and *Tctn2*<sup>-/-</sup> E8.0 nodes stained for AcTub (green), Ninein (red), and DNA (DAPI, blue). Scale bar 5μm. **(b)** SEM of wild type and *Tctn2*<sup>-/-</sup> E8.0 nodes. Scale bar 5μm. **(c)** SEM of wild type and *Tctn2*<sup>-/-</sup> E9.5 neural tubes. Scale bar 0.5μm. **(d)** TEM of wild type and *Tctn2*<sup>-/-</sup> E9.5 neural tubes. Scale bar 0.5μm. **(e)** Sections of E12.5 hindlimb bud mesenchyme stained for AcTub (green) and γ-tubulin (red). Scale bar 10μm. **(f)** Wild type and *Tctn2*<sup>-/-</sup> E9.5 perineural mesenchyme stained for Arl13b (red) and DNA (DAPI, blue). Dotted line marks neural tube border. Scale bar 10μm.

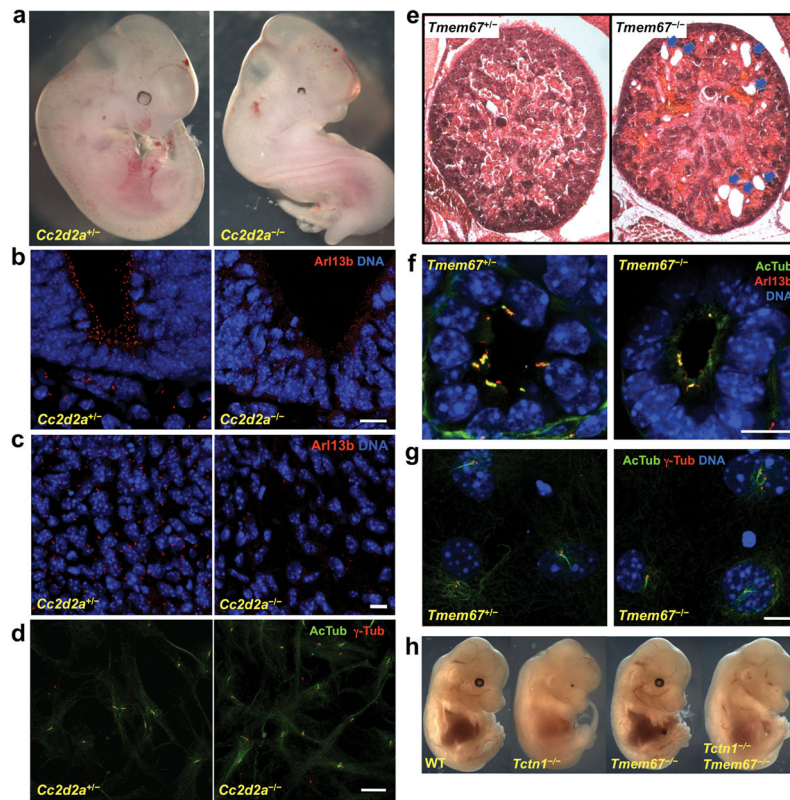


**Figure 5. Tctn1 interactors Cc2d2a and Tmem67 promote ciliogenesis**

(a) Control and *Cc2d2a*<sup>-/-</sup> E10.5 mouse embryo littermates. (b) Control and *Cc2d2a*<sup>-/-</sup> E9.5 ventral neural tube stained for Arl13b (red) and DNA (DAPI, blue). (c) Control and *Cc2d2a*<sup>-/-</sup> E9.5 perineural mesenchyme stained for Arl13b (red) and DNA (DAPI, blue). (d) *Cc2d2a*<sup>-/-</sup> primary MEFs generate cilia, marked by AcTub (green), with associated basal bodies, marked by  $\gamma$ -tubulin (red). (e) Hematoxylin and eosin staining of E18.5 kidney sections from control and *Tmem67*<sup>-/-</sup> embryos. Kidney cysts are visible in the mutant (arrows). (f) Control and *Tmem67*<sup>-/-</sup> E18.5 embryonic kidney tubules stained for AcTub (green), Arl13b (red) and DNA (DAPI, blue). Cilia are less abundant in *Tmem67*<sup>-/-</sup> tubules, but possess Arl13b. (g) *Tmem67*<sup>-/-</sup> primary MEFs generate cilia, as stained for AcTub (green),  $\gamma$ -tubulin (red), and DNA (DAPI, blue). (h) *Tctn1* is epistatic to *Tmem67*. At E14.5, *Tmem67*<sup>-/-</sup> mice are indistinguishable from wild type, and *Tctn1*<sup>-/-</sup> *Tmem67*<sup>-/-</sup> double mutant mice are indistinguishable from *Tctn1*<sup>-/-</sup> mice. Scale bars 10 $\mu$ m.

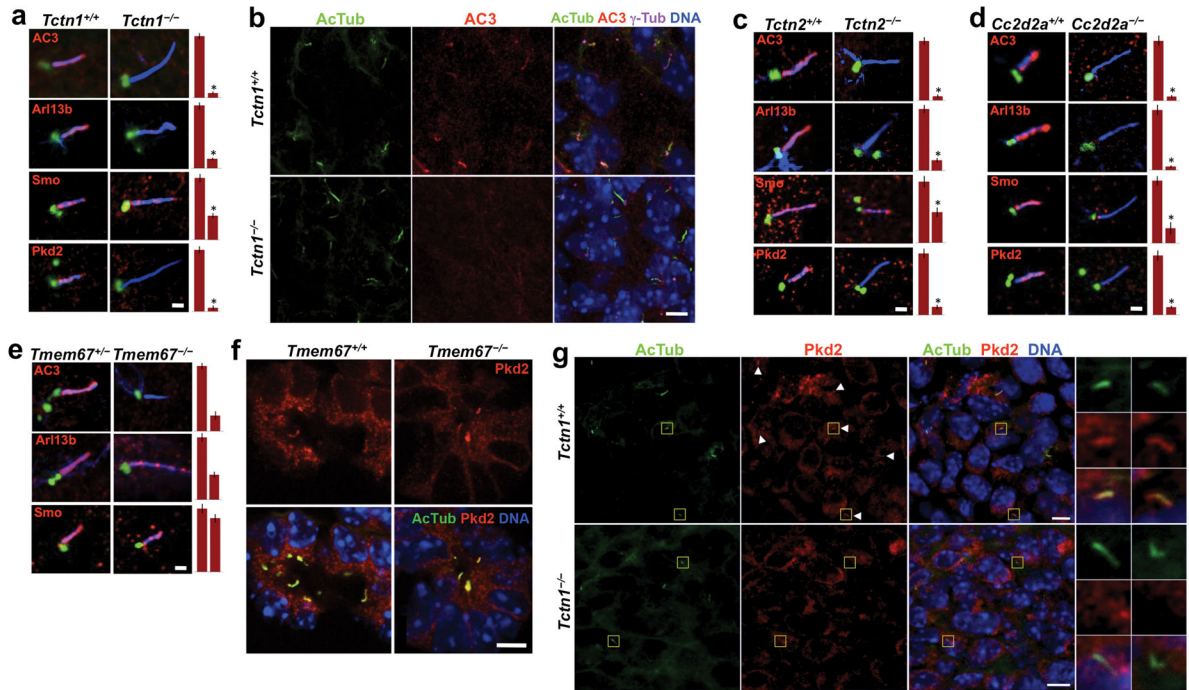


**Figure 6. *Tctn1* and its interactors control the localization of select ciliary membrane proteins**  
**(a)** MEFs from sibling wild type and *Tctn1*<sup>-/-</sup> embryos were stained for AcTub (blue),  $\gamma$ -tubulin (green) and the indicated ciliary proteins (red). Quantifications of the ciliary intensity of these proteins are also shown. Data are shown as mean  $\pm$  SEM. Asterisk denotes statistical significance according to unpaired Student's t-tests (\* = p<0.01). Scale bar 1 $\mu$ m.  
**(b)** E14.5 palatal sections were stained for AcTub, AC3,  $\gamma$ -tubulin and DNA. Ciliary localization of AC3 was evident in wild type embryos, but not in *Tctn1*<sup>-/-</sup> embryos. Scale bar 5 $\mu$ m.  
**(c)** MEFs from sibling wild type and *Tctn2*<sup>-/-</sup> embryos were stained and analyzed as in (a). Scale bar 1 $\mu$ m.  
**(d)** MEFs from sibling wild type and *Cc2d2a*<sup>-/-</sup> embryos were stained and analyzed as in (a). Scale bar 1 $\mu$ m.  
**(e)** MEFs from sibling *Tmem67*<sup>+/-</sup> and *Tmem67*<sup>-/-</sup> embryos were stained and analyzed as in (a). Scale bar 1 $\mu$ m.  
**(f)** E18.5 kidney sections were stained for AcTub, Pkd2 and DNA. Ciliary localization of Pkd2 was evident in both wild type and *Tmem67*<sup>-/-</sup> kidney tubules. Scale bar 10 $\mu$ m.  
**(g)** E14.5 perineural mesenchyme was stained for AcTub, Pkd2 and DNA. Ciliary localization of Pkd2 was evident in wild type embryos, but not in *Tctn1*<sup>-/-</sup> embryos. Boxed regions have been magnified 4X. Scale bars 5 $\mu$ m.

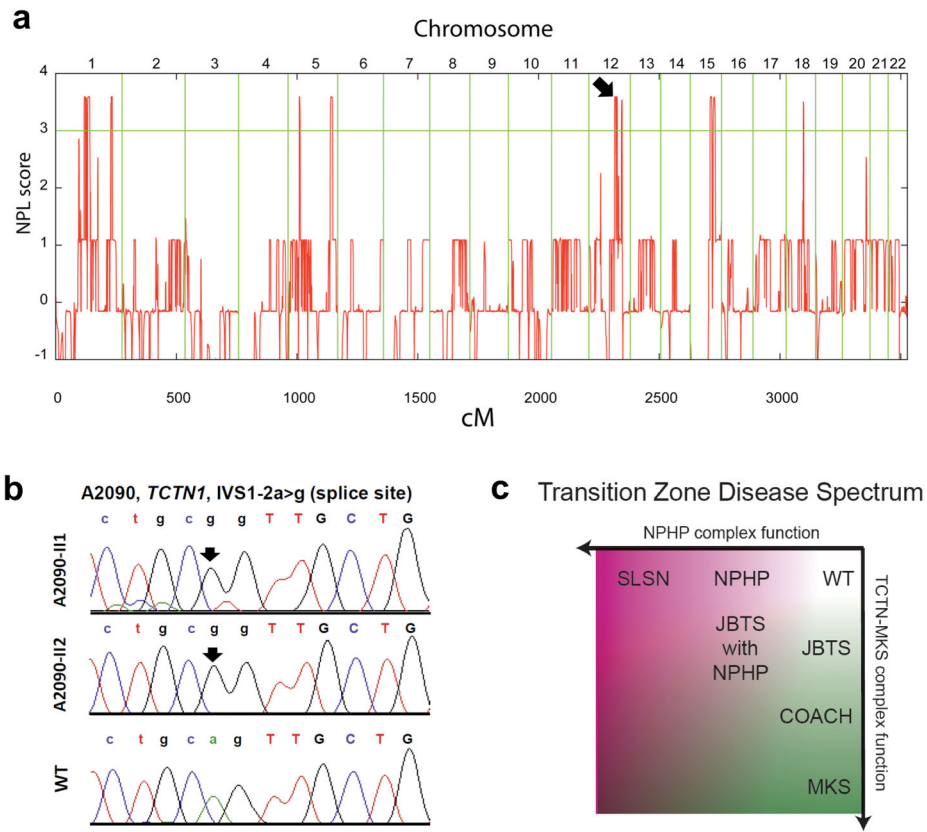


**Figure 7. A human *TCTN1* mutation is a cause of Joubert syndrome**

(a) Non-parametric logarithmic odds score (NPL score) profile across the genomes of two sisters with JBTS of consanguineous family A2090. SNP positions on human chromosomes are concatenated from p-ter (left) to q-ter (right) on the x-axis. Genetic distance is given in cM. Maximum NPL peaks signify regions of homozygosity by descent. A maximum NPL peak on chromosome 12q (arrow) contains the candidate locus *TCTN1*. (b) A homozygous mutation (IVS1-2a>g) of the intron 1 obligatory splice acceptor consensus is present in both siblings (II-1 and II-2) with JBTS of family A2090, but is absent from a healthy control individual (WT). (c) A model of how transition zone dysfunction results in human disease. Progressive compromise of TCTN complex function (y-axis) results in JBTS, COACH and MKS. Progressive compromise of NPHP complex function (x-axis) results in NPHP and SLSN. Mutations that compromise the function of both the TCTN and NPHP complexes may result in syndromes with elements of both, such as JBTS with NPHP.